Journal of Reproduction and Development, Vol. 68, No 4, 2022

Original Article

Differentiation of stem progenitor CD9/SOX2-positive cells is promoted with increased prolactin-producing and endothelial cells in the pituitary

Kotaro HORIGUCHI[1)], Ken FUJIWARA[2)], Takehiro TSUKADA[3)], Takashi NAKAKURA[4)], Saishu YOSHIDA[5)], Rumi HASEGAWA[1)] and Shu TAKIGAMI[1)]

[1)]*Laboratory of Anatomy and Cell Biology, Department of Health Sciences, Kyorin University, Tokyo 181-8612, Japan*
[2)]*Department of Biological Science, Faculty of Science, Kanagawa University, Kanagawa 259-1293, Japan*
[3)]*Department of Biomolecular Science, Faculty of Science, Toho University, Chiba 274-8510, Japan*
[4)]*Department of Anatomy, Graduate School of Medicine, Teikyo University, Tokyo 173-8605, Japan*
[5)]*Department of Biochemistry, The Jikei University School of Medicine, Tokyo 105-8461, Japan*

Abstract. Sex-determining region Y-box 2 (SOX2)-positive cells are stem/progenitor cells in the adenohypophysis, comprising the anterior and intermediate lobes (AL and IL, respectively). The cells are located in the marginal cell layer (MCL) facing Rathke's cleft (primary niche) and the parenchyma of the AL (secondary niche). We previously demonstrated *in vitro* that the tetraspanin superfamily CD9 and SOX2 double-positive (CD9/SOX2-positive) cells in the IL-side MCL migrate to the AL side and differentiate into hormone-producing and endothelial cells in the AL parenchyma. Here, we performed *in vivo* studies to evaluate the role of IL-side CD9/SOX2-positive cells in pregnancy, lactation, and treatment with diethylstilbestrol (DES; an estrogen analog) when an increased population of prolactin (PRL) cells was observed in the AL of the rat pituitary. The proportions of CD9/SOX2-, CD9/Ki67-, and PRL/TUNEL-positive cells decreased in the primary and secondary niches during pregnancy and DES treatment. In contrast, the number of CD9/PRL-positive cells increased in the AL-side MCL and AL parenchyma during pregnancy and during DES treatment. The proportion of PRL/Ki67-positive cells increased in the AL-side MCL and AL parenchyma in response to DES treatment. Next, we isolated CD9-positive cells from the IL-side MCL using an anti-CD9 antibody. During cell culture, the cells formed free-floating three-dimensional clusters (pituispheres). Furthermore, CD9-positive cells in the pituisphere differentiated into PRL cells, and their differentiation potential was promoted by DES. These findings suggest that CD9/SOX2-positive cells in the IL-side MCL may act as adult stem cells in the AL parenchyma that supply PRL cells under the influence of estrogen.
Key words: CD9, Lactotrophs, Pituitary gland, Pregnancy, Stem cells

(**J. Reprod. Dev. 68:** 278–286, 2022)

The pituitary gland plays an important role in reproduction via hormone production. Anatomically, the pituitary gland comprises two different regions: the adenohypophysis and neurohypophysis. The adenohypophysis was further divided into the anterior and intermediate lobes (AL and IL, respectively). The AL contains five types of hormone-producing cells derived from stem/progenitor cells.

In the adenohypophysis, sex-determining region Y-box 2 (SOX2)-positive cells are located along the IL-side and AL-side marginal cell layers (MCLs) facing the Rathke's cleft, which express the binding protein S100β and have been proposed to form the primary stem/progenitor cell niche [1–4]. SOX2-positive cell clusters were present throughout the parenchyma as secondary niches. Recently, we found that cluster of differentiation (CD) 9 and CD81, which are members of the tetraspanin superfamily, are novel specific markers of a subpopulation of SOX2-positive cells in the MCL and parenchymal niches of the rodent pituitary [2]. We successfully isolated CD9-positive cells from IL-side MCL niches using an anti-CD9 antibody with a pluriBead-cascade cell isolation system and found that a subset of isolated CD9- and SOX2-positive (CD9/SOX2-positive) cells in the IL-side MCL could differentiate into endothelial cells and hormone-producing cells of the AL [2, 5–7]. Concurrently, *Cd9* and *Cd81* knockdown in CD9/SOX2-positive cells inhibited prolactin (PRL) cell differentiation. Consistent with these findings, histological observations of the pituitary gland of CD9/CD81-double knockout (CD9/CD81 DKO) mice showed dysgenesis of the IL-side MCL and a reduction in the number of PRL cells in the AL. CD9/CD81 DKO mice also showed infertility [8]. The MCLs of the IL and AL sides were connected at the wedge zone with several bridges formed across them (Supplementary Fig. 1). Recently, we performed *in vitro* chimeric pituitary tissue culture using S100β/GFP transgenic rat [9] and Wistar rat pituitaries and found that CD9/SOX2-positive cells migrate from the IL-side MCL to the AL-side MCL followed by the AL parenchyma through their bridges to supply hormone-producing cells and endothelial cells [5, 10]. PRL and endothelial cells rapidly develop and proliferate during pregnancy and lactation via estrogen-mediated processes. However, it remains unclear how and where PRL and endothelial cells are supplied during reproduction. In addition, the formation of prolactinomas, which are benign pituitary tumors secreting excess prolactin, is accompanied by frequent neo-vasculogenesis and PRL cell proliferation in AL. In animal experiments, prolactinomas have been induced by treatment with diethylstilbestrol (DES), an exogenous estrogen [11–13]. In a previous study, we showed that CD9/SOX2-positive cells migrated and differentiated into endothelial cells during tumorigenesis in rats

Received: April 7, 2022
Accepted: May 23, 2022
Advanced Epub: June 11, 2022

Correspondence: K Horiguchi (e-mail: kota@ks.kyorin-u.ac.jp)

with DES-induced prolactinoma [2]. However, it remains unclear whether CD9/SOX2-positive cells present in the primary niche differentiate into PRL cells in rats with prolactinoma. To address these questions, the present study examined whether CD9/SOX2-positive cells present in the IL-side MCL play an important role in PRL and endothelial cell differentiation during pregnancy, lactation, and DES treatment, when the number of PRL cells is increasing.

Materials and Methods

Animals

Adult Wistar rats were purchased from Japan SLC, Inc. (Shizuoka, Japan). Eight-to-ten-week-old female rats weighing 180–220 g were provided *ad libitum* access to food and water and housed under a 12-h light/dark cycle. Subsequently, the rats were euthanized. The first day on which vaginal spermatozoa were detected was designated as day 0 of pregnancy (P0) and the day of parturition was designated as day 0 of lactation (L0). Estrogen-treated rats were established from male F344 rats. A silastic tube (Kaneka, Osaka, Japan) containing DES (Merck Millipore, Darmstadt, Germany) was subcutaneously implanted in 8-week-old F344 male rats under anesthetization with a combination of medetomidine (0.15 mg/kg; Zenyaku Kogyo, Tokyo, Japan), midazolam (2.0 mg/kg; Sandoz, Tokyo, Japan), and butorphanol (2.5 mg/kg; Meiji Seika Pharma, Tokyo, Japan). The rats were sacrificed 1 week after implantation with a DES tube (DES-1W) by exsanguination from the right atrium after anesthetization. The rats were then perfused with Hanks' balanced salt solution (Thermo Fisher Scientific, Waltham, CA, USA) to isolate CD9-positive cells from the AL and IL or with 4% paraformaldehyde in a 0.05 M phosphate buffer (PB; pH 7.4) to obtain samples for immunohistochemistry. The study protocol was approved by the Committee on Animal Experiments of Kyorin University and was based on the National Institutes of Health Guidelines for the Care and Use of Laboratory Animals.

Immunohistochemistry

The pituitary glands of female rats were removed and immediately immersed in a fixative composed of 4% paraformaldehyde in a 0.05 M PB (pH 7.4) and incubated for 20–24 h at 4°C. The tissues were immersed in PB (pH 7.2) containing 30% sucrose, incubated for more than two days at 4°C, embedded in Tissue Tek O.C.T. compound (Sakura Finetek Japan, Tokyo, Japan), and frozen rapidly. Frozen tissue sections (8 µm-thick) were obtained using a cryostat (Tissue-Tek Polar DM; Sakura Finetek Japan, Co., Ltd., Tokyo, Japan) and mounted on glass slides (Matsunami, Osaka, Japan).

For the double immunofluorescence experiment, frozen sections or cells were incubated overnight at 20–23°C in phosphate-buffered saline (PBS) containing antibodies against CD9 and SOX2 (stem/progenitor cell markers), PRL and Ki67 (proliferation cell marker), and isolectin B4 (endothelial cell marker). The primary and secondary antibodies used are listed in Supplementary Table 1. After washing with PBS, the cells were incubated in PBS containing secondary antibodies. Sections and cells were scanned using a fluorescence microscope (CellSens Dimension System; Olympus, Tokyo, Japan). Each experiment was performed in triplicates. The absence of an observable nonspecific reaction was confirmed using normal mouse and rabbit serum. Nuclei were counterstained by incubation with VECTASHIELD mounting medium containing 4,6-diamidino-2-phenylindole (DAPI; Vector Laboratories, Burlingame, CA, USA). Apoptotic cells were detected via the terminal deoxynucleotidyl transferase dUTP nick-end labeling (TUNEL) assay according to the manufacturer's instructions (*In Situ* Cell Death Detection Kit, Roche, Basel, Switzerland). After the TUNEL assay, the sections were subjected to immunohistochemistry, as described above. Five random fields per slide were imaged using a fluorescence microscope with a 60x objective lens. The number of CD9-positive cells and the total number of cells stained with DAPI per unit area (157.5 × 210 µm^2) were determined using the CellSens Dimension System (Olympus). Observations were performed three times for each experimental group.

Isolation of CD9-immunopositive cells from the AL and IL

Pituitary glands of female Wistar rats at P60 were dissected, and AL was manually separated from the pituitary gland using tweezers. AL and IL/PL tissues were dissected, and the cells were dispersed as described previously [6]. Thereafter, the minced pieces of AL and IL/PL were incubated for 5 min in 1% trypsin (Thermo Fisher Scientific) and 0.2% collagenase containing 5 µg/ml DNase I (Thermo Fisher Scientific) at 37°C. After incubation in Hanks' solution containing 0.3% ethylenediaminetetraacetic acid (FUJIFILM Wako Pure Chemical Corporation Inc., Osaka, Japan) for 5 min at 37°C, the suspension was washed with Hanks' solution. The dispersed cells were counted using a hemocytometer and separated using the Universal Mouse pluriBeads kit (pluriSelect, San Diego, CA, USA), as described in our previous study [6], using mouse monoclonal anti-CD9 antibodies (BD Biosciences, Franklin Lakes, NJ, USA), according to the manufacturer's instructions. CD9-positive and CD9-negative cells were processed for smear preparation, cultivation, and immunocytochemistry analysis. After immunocytochemistry, four random fields (157.5 × 210 µm^2) were captured per slide using a 60-fold objective lens. The number of CD9-positive cells and the total number of cells (stained with DAPI) per unit area were determined using the CellSens Dimension system (Olympus). Cell counts were performed thrice for each experimental group.

Growth and differentiation of pituispheres

CD9-positive cells isolated from the IL were plated on 35 mm untreated dishes (AGC Techno Glass, Shizuoka, Japan) at 20,000 cells/dish in DMEM/F-12 containing B27 supplement (1:50; Thermo Fisher Scientific), N2 supplement (1:100; FUJIFILM Wako Pure Chemical Corporation Inc.), bovine serum albumin (BSA, 0.5%; Sigma-Aldrich), basic fibroblast growth factor (bFGF, 20 ng/ml), and epidermal growth factor (EGF, 20 ng/ml). Cells were incubated in a humidified chamber with 5% CO_2 at 37°C. The pituispheres were passaged by treatment with 0.05% trypsin and 5 mM EDTA in DMEM/F-12 containing 0.5% BSA for 20 min, followed by mechanical dissociation to form a single-cell suspension. This was followed by incubation on 35 mm untreated dishes, as described above, for another 5 days. Pituispheres were collected manually under a microscope using a pipette. The differentiation of pituispheres was induced using an overlay 3D culture on Matrigel-coated 16-well chamber slides (0.4 cm^2/well) (Thermo Fisher Scientific). This was performed using 20 ng/ml bFGF, EGF, and 20% knockout serum replacement (KSR, Thermo Fisher Scientific) for 4 days. The medium was then replaced with a medium containing BIO (GSK3β-inhibitor, 250 nM; FUJIFILM Wako Pure Chemical Corporation Inc.), and the culture was maintained for another 10 days in the presence or absence of DES. More than 10 random spheres/experiments were counted, and three individual experiments were performed.

Statistical analysis

Data are presented as mean ± standard error of the mean of the measured values of at least three preparations for each group of

rats. F-tests and subsequent Student's *t*-tests were performed for two-group comparisons. The Tukey-Kramer test was performed to compare more than two groups. Differences were considered statistically significant at $P < 0.05$.

Results

Detection of SOX2-, PRL-, or isolectin B4-positive cells in the CD9-positive cell population in the MCL and parenchyma of AL

Hematoxylin-eosin staining of the pituitary tissues of Wistar female rats at diestrus, P10, and L20, and of F344 male rats treated with or without DES are shown in Supplementary Fig. 1. The AL area gradually enlarged during pregnancy, lactation, and DES treatment for 1 week (DES-1W). We observed cell bridges across the Rathke's cleft that connect the IL-side and AL-side MCLs (Supplementary Fig. 1, arrowheads). We next stained PRL by immunohistochemistry to quantify the PRL cells in the AL-side MCL and AL parenchyma (Fig. 1A). The proportion of PRL cells at P10 and after DES treatment in the AL-side MCL and at P10, L20, and after DES treatment in the AL parenchyma was significantly higher ($P < 0.01$) than that in diestrus and DES-untreated mice, respectively (Fig. 1B).

We suggest that CD9/SOX2-positive cells migrate sequentially (IL-side MCL, AL-side MCL, and AL parenchyma) by changing their cell properties to those of more committed progenitor cells with the loss of SOX2 expression [10]. CD9/SOX2-positive cells were observed in the IL- and AL-side MCLs and in the AL parenchyma by immunohistochemistry at diestrus (8–10 weeks), P10, L20, and after DES treatment. SOX2-immunopositive signals were detected in the nucleus, and CD9-positive signals were detected in the cell membrane (Fig. 2A). Immunopositive cells were lined along the IL- and AL-side MCLs (Fig. 2A). We counted the number of CD9/SOX2-positive cells and analyzed their proportion among the DAPI-stained cells. At diestrus, the proportion of CD9/SOX2-positive cells was 82.8 (IL-side MCL), 76.7 (AL-side MCL), and 9.3% (parenchyma) (Fig. 2B). This proportion decreased at P10 (Fig. 2B). In the AL-side MCL, the proportion of CD9/SOX2-positive cells also decreased at L20 (Fig. 2B). The proportion of CD9/SOX2-positive cells among DES-treated cells was lower than that of untreated cells (Fig. 2B).

In a previous study, we observed that CD9/PRL-positive cells appeared during the differentiation of CD9/SOX2-positive cells [7]. We identified CD9/PRL-positive cells in the AL-side MCL and the AL parenchyma (Fig. 3A). At diestrus, the proportion of CD9/PRL-positive cells in the AL-side MCL and AL parenchyma was approximately 2.0% and 0.5%, respectively (Fig. 3C). This proportion increased at P10 and L20 (Fig. 3C). Similarly, the proportion of CD9/PRL-positive cells in the AL-side MCL and AL parenchyma increased in the DES treatment group compared with that in the control group (Fig. 3C). These findings indicated that the change in the proportion of CD9/PRL-positive cells was dependent on the induction of PRL expression in CD9-positive cells.

Isolectin B4 is an endothelial cell marker. We have previously shown that CD9-positive cells differentiate into endothelial cells in response to DES [2]. In the present study, we detected isolectin B4-positive endothelial cells in the AL parenchyma at P10 and L20, and after DES-1W (Fig. 3B). Although only a few CD9/isolectin B4-positive cells were observed at diestrus (approximately 0.5%, Fig. 3B and D), the proportion of CD9/isolectin B4-positive cells increased significantly at P10 and L20, and after DES treatment (Fig. 3 D).

Detection of Ki67-positive cells among CD9- or PRL-positive cells in the MCL and parenchyma of AL

Ki67 is a cell proliferation marker. Next, we examined whether PRL cell proliferation was induced by the proliferation of CD9-positive or PRL cells. We quantified the numbers of CD9/Ki67- (Fig. 4A) and PRL/Ki67-positive cells (Fig. 4B). In the IL-side MCL, the proportion of CD9/Ki67-positive cells decreased at P10 and after DES

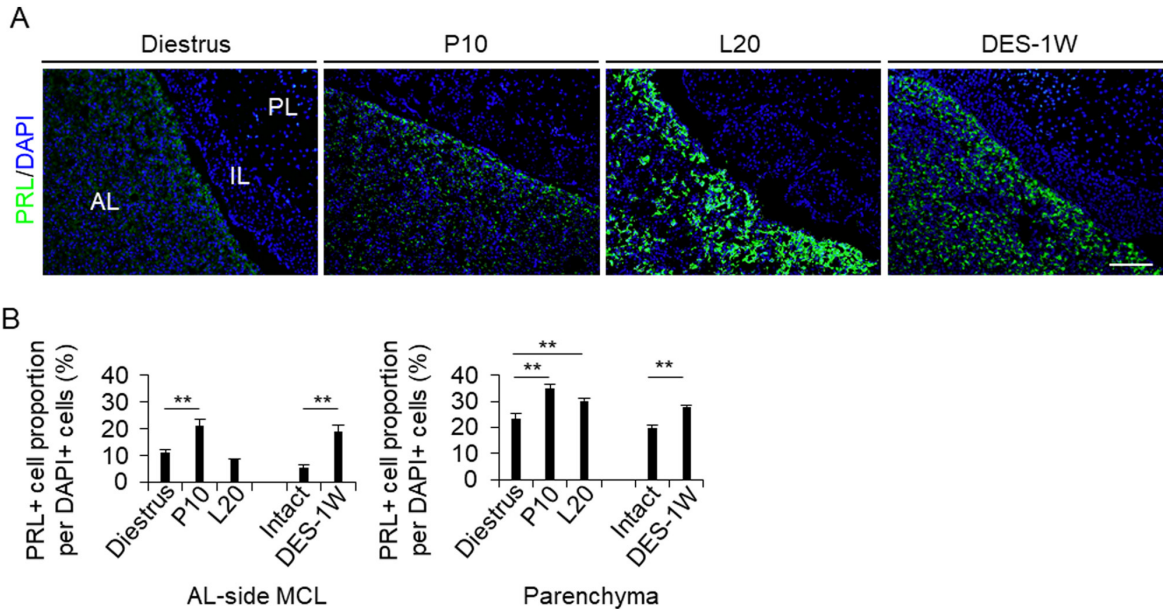

Fig. 1. Proportion of PRL cells in the AL-side MCL and AL parenchyma. (A) Immunohistochemistry for PRL at diestrus (8–10-week-old female rats (Diestrus)), 10 days of pregnancy (P10), and 20 days of lactation (L20) and after 1 week of DES treatment (DES-1W). Images for PRL immunoreactivity (*green*) and DAPI staining (*blue*) are merged. (B) The proportion of PRL cells per DAPI-positive cell in the AL-side MCL (AL-side MCL) and AL parenchyma (Parenchyma). AL, anterior lobe; IL, intermediate lobe; PL, posterior lobe. Scale bar: 200 μm.

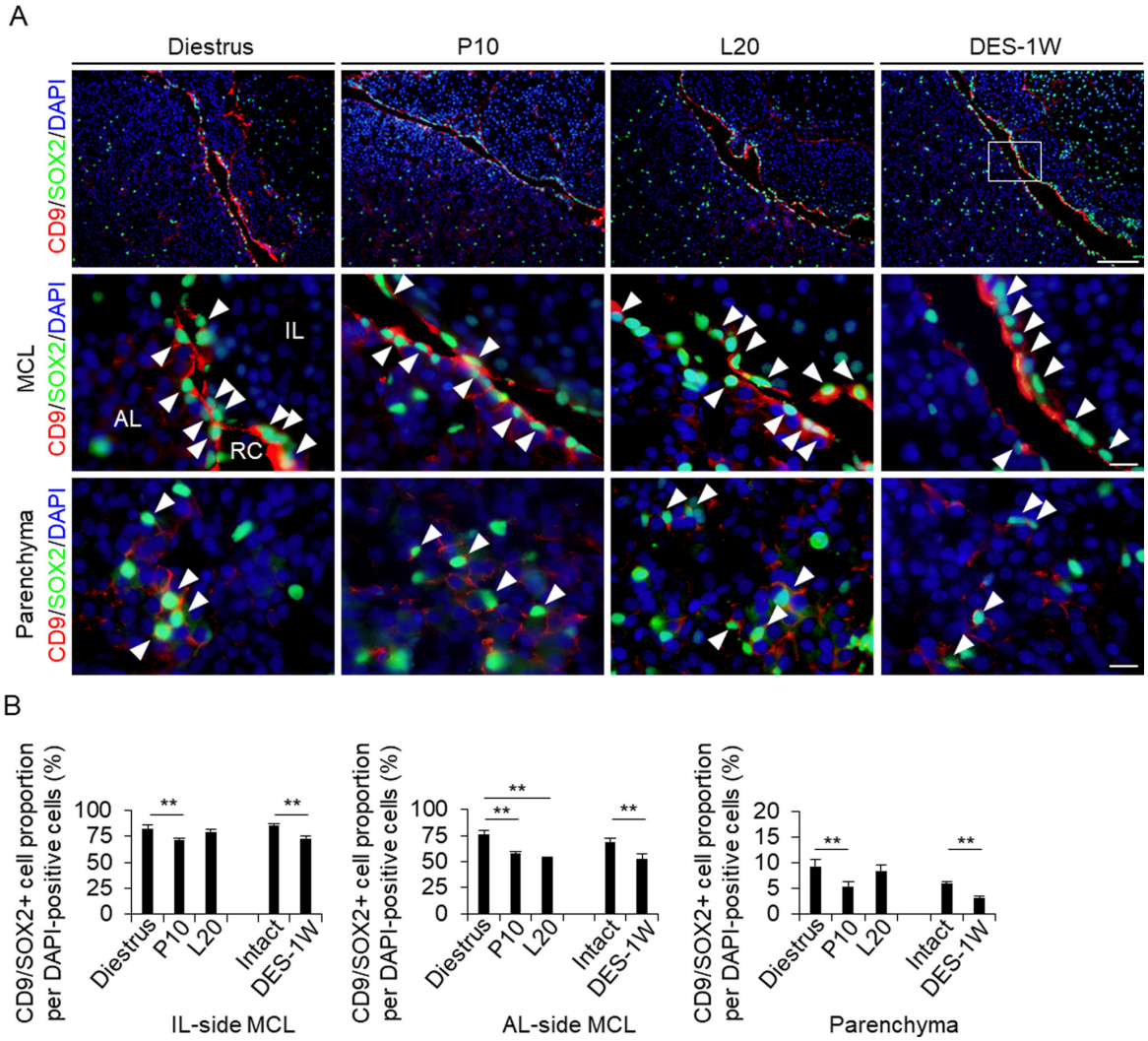

Fig. 2. Detection of CD9/SOX2- and CD9/PRL-positive cells in the IL-side and AL-side MCLs and AL parenchyma. (A) Double immunohistochemistry for CD9 and SOX2 at diestrus (8–10-week-old female rats (Diestrus)), 10 days of pregnancy (P10), and 20 days of lactation (L20) and after 1 week of DES treatment (DES-1W). Merged image of CD9 and SOX2 immunohistochemistry and DAPI staining are shown (First row: low magnification image of pituitary, second row: magnified view of the MCL, third row: magnified views of the parenchyma). White arrowheads indicate CD9/SOX2-positive cells. (B) The proportion of CD9/SOX2-positive cells per DAPI-positive cells in Diestrus, P10, and L20, DES-untreated rats (Intact), and DES-1W in the IL-side MCL, AL-side MCL, and AL parenchyma (Parenchyma). AL, anterior lobe; IL, intermediate lobe; RC: Rathke's cleft. Scale bars: 200 μm (first row of A) and 20 μm (second and third rows of A). ** $P < 0.01$.

treatment compared to those at diestrus and without DES treatment, respectively (Figs. 4A and 5A). In the AL-side MCL, the proportion of CD9/Ki67- and PRL/Ki67-positive cells decreased at P10 and L20 (Figs. 4A, 4 B, 5A, and 5 B). However, the proportion increased in the DES treatment group compared to that in the untreated group (Fig. 5B). In the AL parenchyma, the proportion of PRL/Ki67-positive cells decreased at P10 and L20 compared to that at diestrus (Figs. 4B and 5 B), while the number of CD9/Ki67-positive cells decreased at P10, but not at L20 (Figs. 4B and 5 B). The proportion of PRL/Ki67-positive cells was higher in the DES treatment group than in the untreated group (Fig. 5B).

Observation of apoptotic cells in the MCL and parenchyma of AL

To detect apoptosis in PRL cells, we performed a TUNEL assay. We counted the number of TUNEL-positive cells in the AL parenchyma at diestrus, P10, L20, and after DES treatment (Figs. 4C and 5C). The proportions of TUNEL- and PRL/TUNEL-positive cells decreased at P10 and L20 in the DES-treated group compared with those at diestrus and in the DES-untreated group, respectively (Fig. 5C).

Purification and characterization of CD9-positive cells from the AL

To observe the cells *in vitro* during the process of differentiation with CD9 expression, we purified CD9-positive cells from the AL using a monoclonal anti-rat CD9 antibody with the pluriBead-cascade cell isolation system. Isolated CD9-positive and CD9-negative cell fractions were processed for smear preparation and were used for CD9 immunocytochemistry. The proportion of CD9-immunopositive cells in the CD9-positive fraction was 92.8% (Fig. 6A). We used double immunocytochemistry to detect CD9, PRL, or isolectin-B4. We detected CD9/PRL-positive and CD9/isolectin-B4-positive cells in the CD9-positive cell population (Fig. 6B), and their proportions were both 0.7% (Fig. 6B).

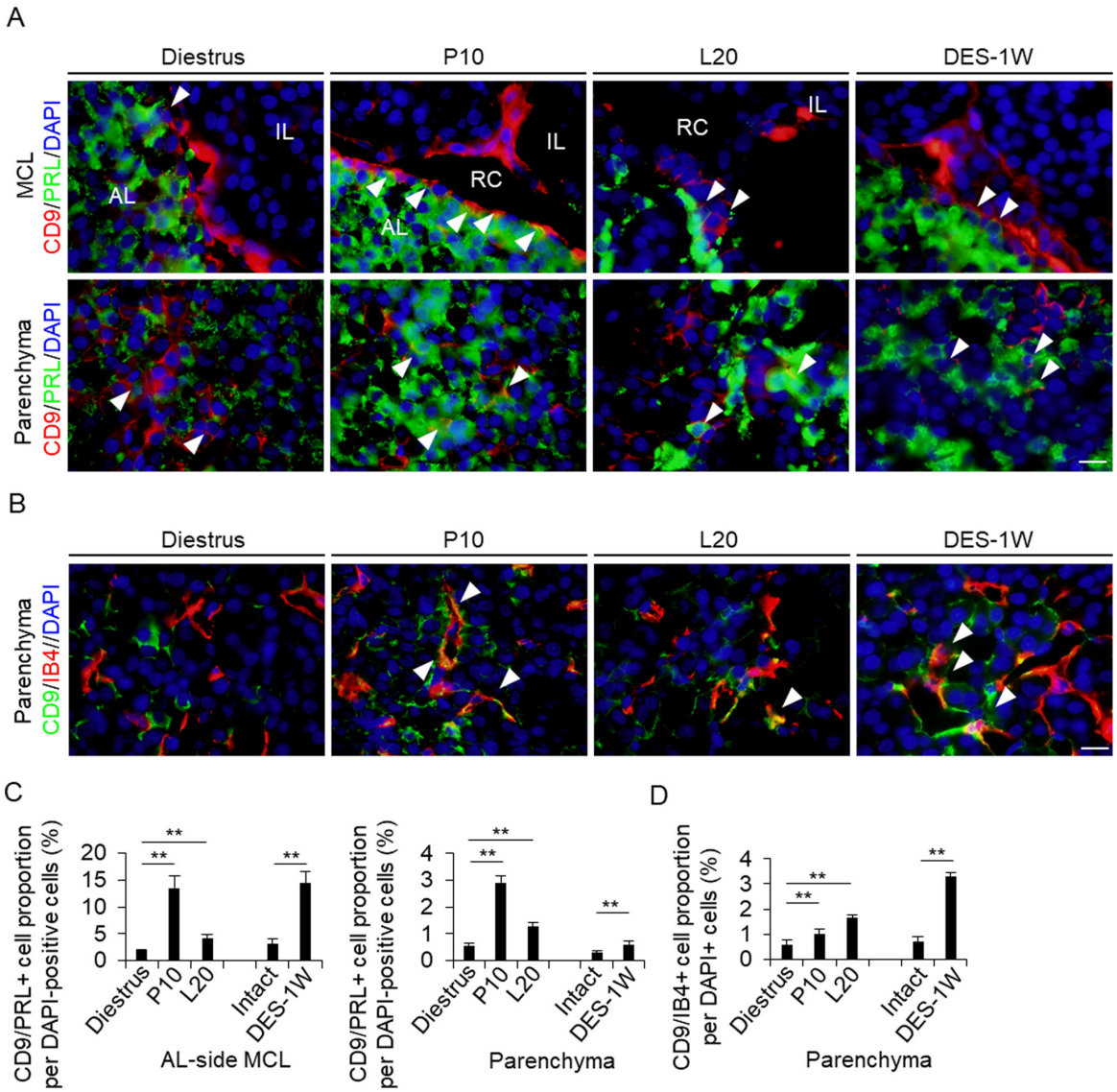

Fig. 3. Detection of CD9/PRL-positive cells and endothelial cells in the IL- and AL-side MCLs and AL parenchyma. (A) Double immunohistochemistry for CD9 and PRL at diestrus (8–10-week-old female rats (Diestrus)), 10 days of pregnancy (P10), and 20 days of lactation (L20) and after 1 week of DES treatment (DES-1W). Merged image of CD9 (*red*) and PRL (*green*) immunohistochemistry and DAPI staining (*blue*) are shown. (B) Immunohistochemistry for CD9 and isolectin-B4 (IB4) at Diestrus, P10, and L20 and DES-1W. Merged images of CD9 (*green*) and IB4 (*red*) immunohistochemistry with DAPI staining (*blue*) are shown. White arrowheads indicate CD9/PRL- and CD9/IB4-positive cells. (C and D) The proportion of CD9/PRL- (C) or CD9/IB4-positive cells (D) per DAPI-positive cells in Diestrus, P10, L20, DES-untreated rats (Intact), and DES-1W in the AL-side MCL and AL parenchyma (Parenchyma). AL, anterior lobe; IL, intermediate lobe; MCL, marginal cell layer; PL, posterior lobe; PRL, prolactin; RC: Rathke's cleft. Scale bars: 20 μm (A and B). ** $P < 0.01$.

Effect of estrogen on pituisphere differentiation

It is widely known that blood estrogen concentration increases during pregnancy. Estrogen is associated with the differentiation of CD9-positive cells in the AL into PRL cells [5]. We examined whether estrogen affects the differentiation of the pituisphere composed of CD9-positive cells from the IL-side MCL. We stained the estrogen receptor alpha (ERα) in CD9-positive cells using immunohistochemistry (Fig. 6C). CD9-positive cells in the MCL and AL parenchyma were immunopositive for ERα (Fig. 6C). We purified CD9-positive cells from IL-side MCL using the pluriBead-cascade cell isolation system. Isolated CD9-positive and CD9-negative cell fractions were processed for smear preparation and were used for CD9 immunocytochemistry. The proportion of CD9-positive cells in the CD9-positive fraction from the IL-side MCL was 96.1% (Fig. 6D). Figure 6E shows the pituisphere formed from IL-side CD9-positive cells after 5-day cultivation. To compare the differentiation ability of PRL cells treated with or without DES, PRL immunocytochemistry was performed after the 14-day cultivation of the cells in differentiation media. Intriguingly, PRL cells were detected in IL-side pituispheres (Fig. 6E), and their numbers were higher in the DES-treated group than in the untreated group (Fig. 6F).

Discussion

In the present study, we showed that the proportions of CD9/SOX2-positive cells and CD9/Ki67-positive cells in IL- and AL-side MCLs and AL parenchyma decreased during pregnancy and after DES treatment. The proportion of PRL/Ki67-positive cells

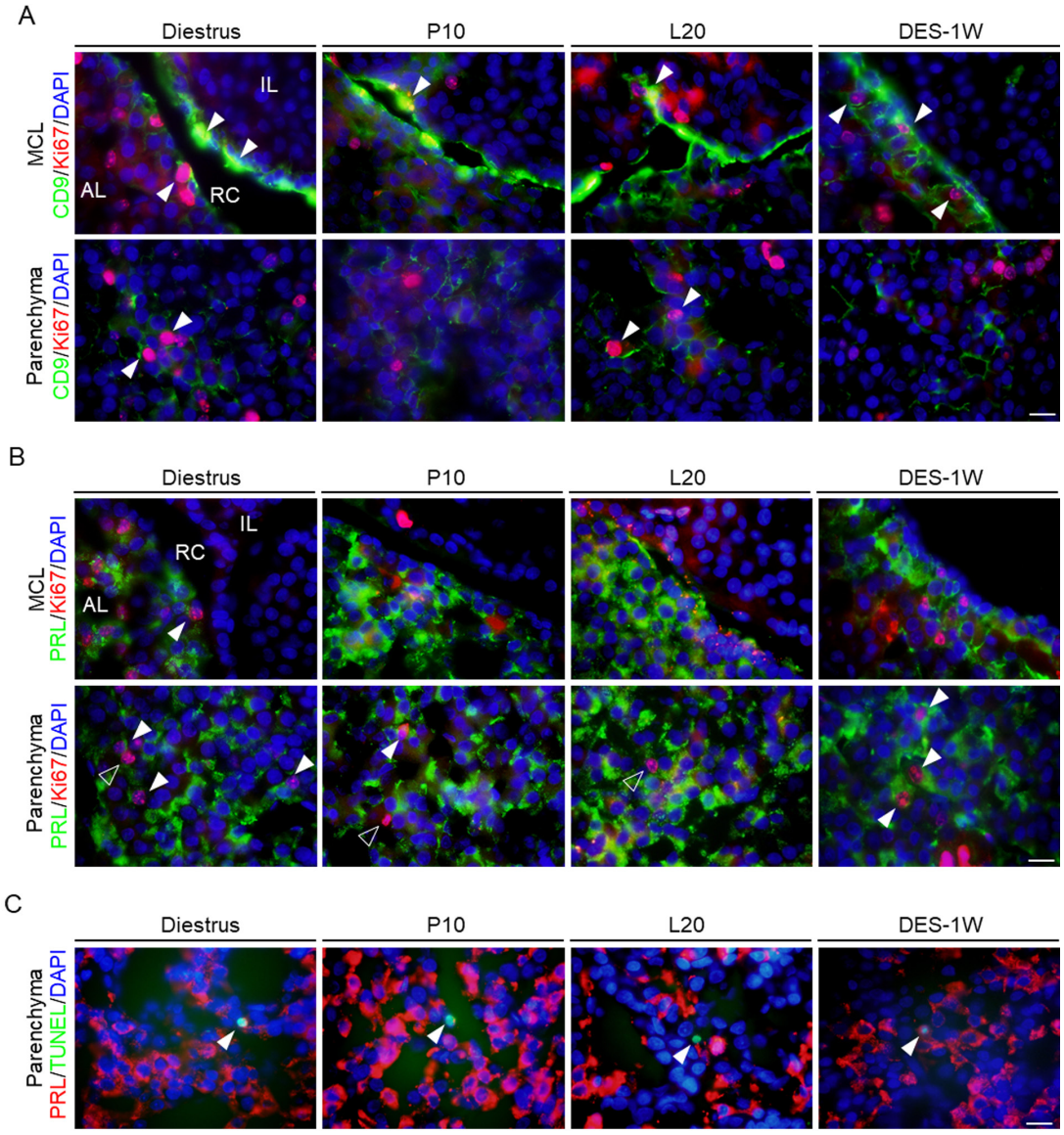

Fig. 4. Observation of CD9/Ki67- and PRL/Ki67-positive cells in the IL-side and AL-side MCLs and AL parenchyma. (A) Double immunohistochemistry for CD9 and Ki67 at diestrus (8–10-week-old female rats (Diestrus)), 10 days of pregnancy (P10), and 20 days of lactation (L20) and after 1 week of DES treatment (DES-1W). Merged image of Ki67 (*red*) and CD9 (*green*) immunohistochemistry and DAPI staining (*blue*) in the MCL (first row) and parenchyma (second row) are shown. (B) Double immunohistochemistry for PRL and Ki67 at Diestrus, P10, L20, and DES-1W. Merged images of Ki67 (*red*) and PRL (*green*) immunohistochemistry and DAPI staining (*blue*) in the MCL (first row) and parenchyma (second row) are shown. White arrowheads indicate CD9/Ki67- or PRL/Ki67-positive cells. (C) TUNEL assay with PRL immunohistochemistry at the parenchyma in Diestrus, P10, L20, DES-untreated rats (Intact), and DES-1W. TUNEL assay (*green*) and immunohistochemistry for PRL (*red*) with DAPI staining (*blue*) are shown. AL, anterior lobe; IL, intermediate lobe; TUNEL, terminal deoxynucleotidyl transferase dUTP nick-end labeling. Scale bars: 20 μm (A–C).

in the AL-side MCL and AL parenchyma also decreased during pregnancy. In contrast, the proportions of CD9/PRL-positive and CD9/IB-4-positive cells in the AL-side MCL and AL parenchyma increased during pregnancy and after DES treatment. The number of PRL/Ki67-positive cells in the AL-side MCL and AL parenchyma also increased following DES treatment. We also confirmed that the differentiation of CD9-positive cells into PRL cells in the IL-side MCL was induced by estrogen.

The proportion of PRL cells in the AL increases from 15 to 20% to approximately 50% of the total pituitary cell population during pregnancy and lactation [14–17]. However, the cells from which PRL cells are derived remain unknown. In a recent study, we showed the possibility that CD9/SOX2-positive cells from the IL-side MCL supply PRL cells to the AL [5]. We also showed that CD9/PRL-positive cells in the sphere formed from CD9/SOX2-positive cells in the AL and IL [5, 7]. In the present study, we demonstrated changes in CD9/SOX2- and CD9/PRL-positive cell proportions in female rats during pregnancy and lactation. The number of CD9/SOX2-positive cells decreased in the IL- and AL-side MCLs and parenchyma during pregnancy. In contrast, the number of CD9/PRL-positive cells in AL parenchyma increased. These findings suggest that during pregnancy, PRL-positive cells may be formed from CD9/SOX2-positive stem/progenitor cells in the IL-side MCL. Similarly, we observed that the number of CD9/IB4-positive cells

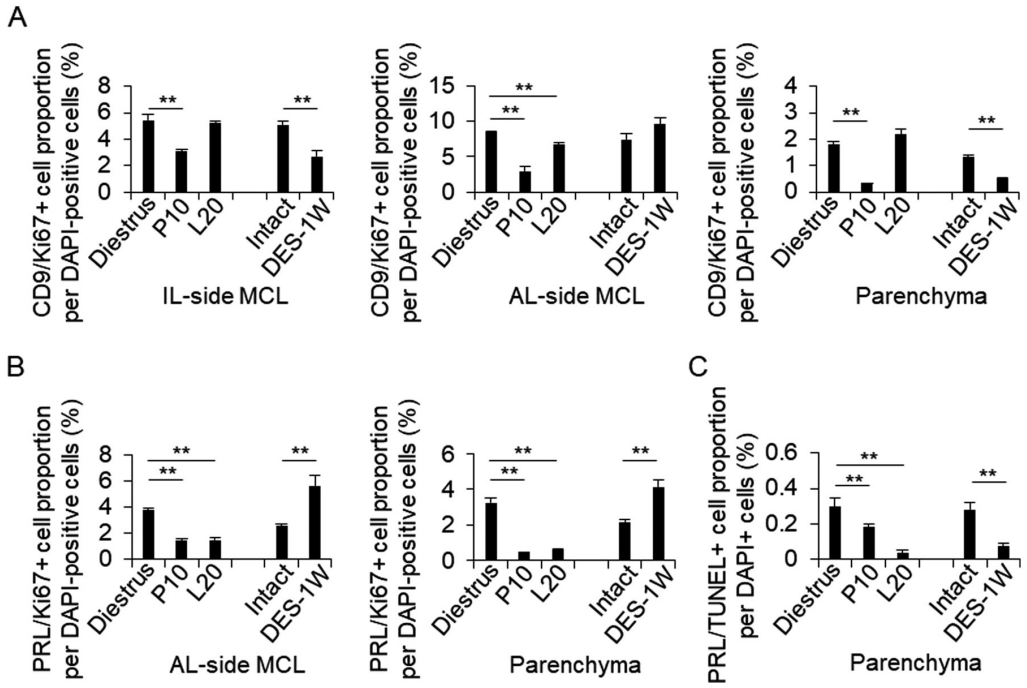

Fig. 5. The proportion of CD9/Ki67- and PRL/Ki67-positive cells in the IL-side and AL-side MCLs and AL parenchyma. (A–C) The proportion of CD9/Ki67- (A), PRL/Ki67- (B), and PRL/TUNEL-positive cells (C) per DAPI-positive cells in Diestrus, P10, L20, DES-untreated rats (Intact), and DES-1W at the IL-side MCL, AL-side MCL, and AL parenchyma (Parenchyma). ** $P < 0.01$.

in AL increased during pregnancy and lactation. Estrogen and PRL induce vascularization of the pituitary gland [18]. In a recent study, we showed that cultured CD9-positive cells from the AL form a capillary-like network and are immunopositive for endothelial cell markers [2]. Similar to CD9/PRL-positive cells, CD9/IB4-positive endothelial cells may be derived from CD9/SOX2-positive cells. Our recent study showed the formation of a cell bridge across Rathke's cleft between the IL and AL and the migration of CD9/SOX2-positive cells from the IL-side MCL into the AL-side MCL [10]. Furthermore, CD9/SOX2-positive cells from the IL-side MCL showed higher expression of stem cell markers (*Sox2* and *S100b*) and pituisphere-forming capacity than those from the AL-side MCL [5], suggesting that CD9/SOX2-positive cells migrate sequentially (IL-side MCL, AL-side MCL, and AL parenchyma) by changing their cell properties to those typically observed in committed progenitor cells and eventually differentiate into PRL cells or endothelial cells in the AL parenchyma during pregnancy and lactation.

In the present study, we successfully isolated CD9-positive cells from the IL-side MCL and AL containing the AL-side MCL and parenchyma. The proportions of CD9/PRL-positive and CD9/IB4-positive cells in the CD9-positive fraction of AL were approximately 0.7%. Consistently, in diestrus, the proportions of CD9/PRL-positive and CD9/IB4-positive cells per unit of total cells were approximately 0.5%. These results suggest that less than 1% of CD9/SOX2-positive cells contribute to hormone-producing and endothelial cell differentiation in normal AL. However, during pregnancy and lactation, we found that the proportion of CD9/PRL-positive cells increased to 13 and 3% in the AL-side MCL and AL parenchyma, respectively, suggesting that an increase in the number of PRL cells during pregnancy and lactation is attributed to an increased supply of CD9/SOX2-positive cells.

The present study also evaluated the effects of apoptosis on the PRL cell population during pregnancy and lactation. Although the proportion of apoptotic cells significantly decreased in the AL parenchyma, the reductions were subtle, from 0.3% (diestrus) to 0.2% (pregnancy) and 0.05% (lactation). Therefore, the increased number of PRL cells during pregnancy and lactation may be due to the differentiation of CD9/SOX2-positive cells in the AL after migration from the IL-side MCL. However, as the proportion of CD9/Ki67-positive cells in the IL-side MCL decreased, it is still unclear how the CD9/SOX2-positive cells in the IL-side MCL supply PRL cells to the AL during pregnancy and lactation, while their self-proliferation activity is low. Some reports show migration of stem/progenitor cells from outside the pituitary gland [19–21], however, further analysis is needed to identify the origin of CD9/SOX2-positive cells in the IL-side MCL.

Estrogen is required for the proliferation and differentiation of PRL cells from CD9/SOX2-positive cells in the AL parenchyma [5]. In the present study, the proportion of PRL/Ki67-positive cells increased with DES treatment but decreased during pregnancy and lactation. This difference may be due to the difference between physiological (corresponding to pregnancy and lactation) and pathological (corresponding to DES treatment) tissues. Some factors, such as higher levels of progesterone or placental lactogen during pregnancy and lower levels of estrogen during lactation, may be associated with the process that prevents neoplastic transformation of PRL cells during pregnancy and lactation. Further studies are needed to confirm this hypothesis.

In conclusion, PRL cells were derived from CD9/SOX2-positive cells in IL-side MCL during pregnancy and lactation. Estrogen also triggers the differentiation and proliferation of PRL cells in male rats. These findings provide a clear understanding of one of the mechanisms by which PRL cells form from adult stem/progenitor cells and may be of relevance in future studies on other hormone-producing cells in the pituitary.

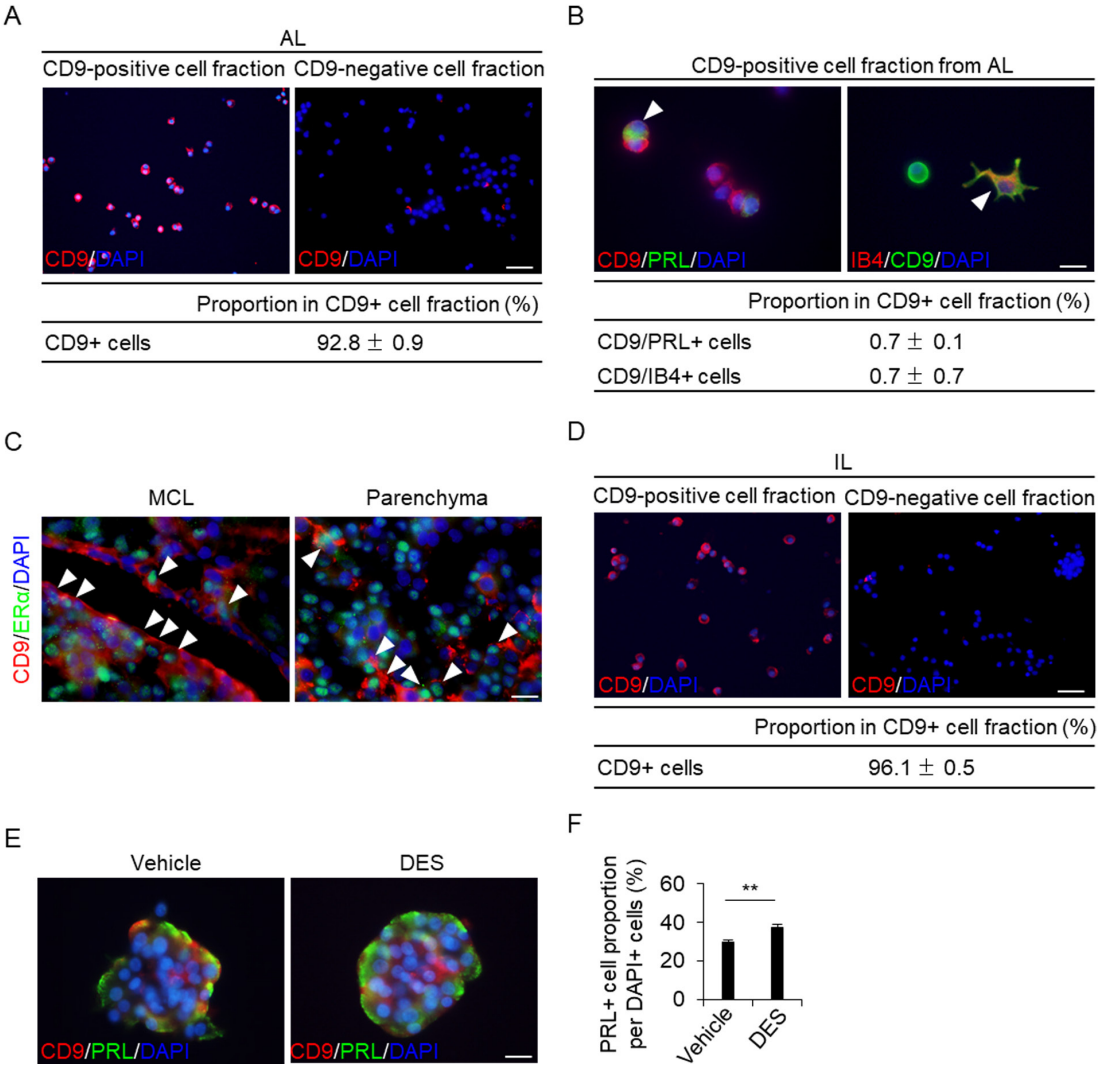

Fig. 6. Isolation of CD9-positive cells from the AL or IL of female rats. (A) CD9 immunofluorescence (*red*) and DAPI staining (*blue*) in a smear preparation of a CD9-positive fraction. The proportions of CD9-positive (CD9+) cells in CD9-positive fractions separated using pluriBeads are indicated (mean ± SEM, n = 3). The number of DAPI-positive and immunopositive cells was counted in random areas of the smear preparations, and the proportion of CD9-positive cells was calculated. (B) Immunofluorescence staining for CD9 and PRL or isolectin-B4 (IB4) in the CD9-positive fraction cultured for 72 h. The table shows the proportion of CD9/PRL-positive (CD9/PRL+) and CD9/IB4-positive (CD9/IB4+) cells. (C) Double immunohistochemistry for CD9 and Erα at Diestrus, P10, L20, and DES-1W. Merged images of CD9 (*red*) and ERα (*green*) immunohistochemistry and DAPI staining (*blue*) in the MCL (left row) and parenchyma (right row) are shown. White arrowheads indicate CD9/ERα-positive cells. (D) CD9 immunofluorescence (*red*) and DAPI staining (*blue*) in a smear preparation of a CD9-positive fraction from the IL-side MCL. The proportions of CD9-positive (CD9+) cells in the CD9-positive fractions separated using pluriBeads are indicated (mean ± SEM, n = 3). (E) Double immunofluorescence staining for CD9 and PRL with vehicle or DES in a pituisphere formed using IL-side MCL CD9-positive cells. (F) The proportion of PRL-positive cells in the pituispheres formed by IL-side MCL CD9-positive cells. AL, anterior lobe; DES, diethylstilbestrol; IL, intermediate lobe; MCL, marginal cell layer; PRL, prolactin. ** $P < 0.01$. Scale bars: 50 μm (A and D), 20 μm (C), and 10 μm (B and E).

Conflict of interests: The authors have no conflicts of interest to declare that might affect the impartiality of this study.

Acknowledgements

We thank the Joint Usage/Research Center for Endocrinine/Metabolism, Institute for Molecular and Cellular Regulation, Gunma University (www.imcr.gunma-u.ac.jp/activity/activity3) for providing antibodies. We would like to thank Editage (www.editage.jp) for English language editing. This study was supported by grants from JSPS KAKENHI (grant no. 22K06798 to K.H.).

References

1. **Fauquier T, Rizzoti K, Dattani M, Lovell-Badge R, Robinson IC.** SOX2-expressing progenitor cells generate all of the major cell types in the adult mouse pituitary gland. *Proc Natl Acad Sci USA* 2008; **105**: 2907–2912. [Medline] [CrossRef]
2. **Horiguchi K, Fujiwara K, Yoshida S, Nakakura T, Arae K, Tsukada T, Hasegawa R, Takigami S, Ohsako S, Yashiro T, Kato T, Kato Y.** Isolation and characterisation of CD9-positive pituitary adult stem/progenitor cells in rats. *Sci Rep* 2018; **8**: 5533. [Medline] [CrossRef]
3. **Vankelecom H, Chen J.** Pituitary stem cells: where do we stand? *Mol Cell Endocrinol* 2014; **385**: 2–17. [Medline] [CrossRef]
4. **Yoshida S, Nishimura N, Ueharu H, Kanno N, Higuchi M, Horiguchi K, Kato T, Kato Y.** Isolation of adult pituitary stem/progenitor cell clusters located in the parenchyma of the rat anterior lobe. *Stem Cell Res (Amst)* 2016; **17**: 318–329. [Medline] [CrossRef]
5. **Horiguchi K, Fujiwara K, Takeda Y, Nakakura T, Tsukada T, Yoshida S, Hasegawa R, Takigami S, Ohsako S.** CD9-positive cells in the intermediate lobe of the pituitary

gland are important supplier for prolactin-producing cells in the anterior lobe. *Cell Tissue Res* 2021; **385**: 713–726. [Medline] [CrossRef]

6. **Horiguchi K, Fujiwara K, Yoshida S, Tsukada T, Hasegawa R, Takigami S, Ohsako S, Yashiro T, Kato T, Kato Y.** CX3CL1/CX3CR1-signalling in the CD9/S100β/SOX2-positive adult pituitary stem/progenitor cells modulates differentiation into endothelial cells. *Histochem Cell Biol* 2020; **153**: 385–396. [Medline] [CrossRef]
7. **Horiguchi K, Yoshida S, Tsukada T, Fujiwara K, Nakakura T, Hasegawa R, Takigami S, Ohsako S.** Cluster of differentiation (CD) 9-positive mouse pituitary cells are adult stem/progenitor cells. *Histochem Cell Biol* 2021; **155**: 391–404. [Medline] [CrossRef]
8. **Jin Y, Takeda Y, Kondo Y, Tripathi LP, Kang S, Takeshita H, Kuhara H, Maeda Y, Higashiguchi M, Miyake K, Morimura O, Koba T, Hayama Y, Koyama S, Nakanishi K, Iwasaki T, Tetsumoto S, Tsujino K, Kuroyama M, Iwahori K, Hirata H, Takimoto T, Suzuki M, Nagatomo I, Sugimoto K, Fujii Y, Kida H, Mizuguchi K, Ito M, Kijima T, Rakugi H, Mekada E, Tachibana I, Kumanogoh A.** Double deletion of tetraspanins CD9 and CD81 in mice leads to a syndrome resembling accelerated aging. *Sci Rep* 2018; **8**: 5145. [Medline] [CrossRef]
9. **Itakura E, Odaira K, Yokoyama K, Osuna M, Hara T, Inoue K.** Generation of transgenic rats expressing green fluorescent protein in S-100beta-producing pituitary folliculo-stellate cells and brain astrocytes. *Endocrinology* 2007; **148**: 1518–1523. [Medline] [CrossRef]
10. **Horiguchi K, Fujiwara K, Tsukada T, Nakakura T, Yoshida S, Hasegawa R, Takigami S, Ohsako S.** CD9-positive cells in the intermediate lobe migrate into the anterior lobe to supply endocrine cells. *Histochem Cell Biol* 2021; **156**: 301–313. [Medline] [CrossRef]
11. **De Nicola AF, von Lawzewitsch I, Kaplan SE, Libertun C.** Biochemical and ultrastructural studies on estrogen-induced pituitary tumors in F344 rats. *J Natl Cancer Inst* 1978; **61**: 753–763. [Medline]
12. **Fujiwara K, Davaadash B, Yatabe M, Kikuchi M, Horiguchi K, Kusumoto K, Kouki T, Yashiro T.** Reduction of retinaldehyde dehydrogenase 1 expression and production in estrogen-induced prolactinoma of rat. *Med Mol Morphol* 2008; **41**: 126–131. [Medline] [CrossRef]
13. **Holtzman S, Stone JP, Shellabarger CJ.** Influence of diethylstilbestrol treatment on prolactin cells of female ACI and Sprague-Dawley rats. *Cancer Res* 1979; **39**: 779–784. [Medline]
14. **Asa SL, Penz G, Kovacs K, Ezrin C.** Prolactin cells in the human pituitary. A quantitative immunocytochemical analysis. *Arch Pathol Lab Med* 1982; **106**: 360–363. [Medline]
15. **Goluboff LG, Ezrin C.** Effect of pregnancy on the somatotroph and the prolactin cell of the human adenohypophysis. *J Clin Endocrinol Metab* 1969; **29**: 1533–1538. [Medline] [CrossRef]
16. **Scheithauer BW, Sano T, Kovacs KT, Young WF Jr, Ryan N, Randall RV.** The pituitary gland in pregnancy: a clinicopathologic and immunohistochemical study of 69 cases. *Mayo Clin Proc* 1990; **65**: 461–474. [Medline] [CrossRef]
17. **Stefaneanu L, Kovacs K, Lloyd RV, Scheithauer BW, Young WF Jr, Sano T, Jin L.** Pituitary lactotrophs and somatotrophs in pregnancy: a correlative in situ hybridization and immunocytochemical study. *Virchows Arch B Cell Pathol Incl Mol Pathol* 1992; **62**: 291–296. [Medline] [CrossRef]
18. **Elias KA, Weiner RI.** Direct arterial vascularization of estrogen-induced prolactin-secreting anterior pituitary tumors. *Proc Natl Acad Sci USA* 1984; **81**: 4549–4553. [Medline] [CrossRef]
19. **Horiguchi K, Yako H, Yoshida S, Fujiwara K, Tsukada T, Kanno N, Ueharu H, Nishihara H, Kato T, Yashiro T, Kato Y.** S100β-positive cells of mesenchymal origin reside in the anterior lobe of the embryonic pituitary gland. *PLoS One* 2016; **11**: e0163981. [Medline] [CrossRef]
20. **Ueharu H, Yoshida S, Kanno N, Horiguchi K, Nishimura N, Kato T, Kato Y.** SOX10-positive cells emerge in the rat pituitary gland during late embryogenesis and start to express S100β. *Cell Tissue Res* 2018; **372**: 77–90. [Medline] [CrossRef]
21. **Ueharu H, Yoshida S, Kikkawa T, Kanno N, Higuchi M, Kato T, Osumi N, Kato Y.** Gene tracing analysis reveals the contribution of neural crest-derived cells in pituitary development. *J Anat* 2017; **230**: 373–380. [Medline] [CrossRef]